Exposure of highly reflective Far-Ultraviolet Coatings to LEO environment for TRL advancement for the Habitable Worlds Observatory

Manuel A. Quijada[a], Luis V. Rodriguez de Marcos[a,b], Javier G. Del Hoyo[a], Andrew Howe[a], Mateo F. Batkis[a], Edward J. Wollack[a], Breann Sitarski[a], John Hennessy[c], David Boris[d], and Scott Walton[d]

[a]NASA Goddard Space Flight Center, Code 551, Greenbelt, MD 20771
[b]Catholic University of America, Washington DC 20064
[c]Jet Propulsion Laboratory, California Institute of Technology, Pasadena, CA 91109
[d]U.S. Naval Research Laboratory, Washington, DC 20375

ABSTRACT

Over the past several years, our team at the NASA Goddard Space Flight Center (GSFC), in collaboration with the Jet Propulsion Laboratory (JPL) and the Naval Research Laboratory (NRL), have developed several new protected Al coating technologies with improved Far-Ultraviolet (FUV) reflectance performance and more robust environmental stability. These include Al protected with lithium-based fluoride (LiF) coatings such as hot-deposited LiF (eLiF), XeF_2-passivated LiF coatings (XeLiF), Li_3AlF_6 overcoats, AlF_3 (plasma passivated), and XeF_2 passivated MgF_2 coatings ($XeMgF_2$). However, despite these developments, relatively little experimental information exists regarding the long-term stability of these coatings after simultaneous exposure to the Low Earth Orbit (LEO) environment. To evaluate their environmental durability and advance their Technology Readiness Level (TRL), representative samples of these coating technologies, Al+XeLiF, Al+eLiF, Al+Li_3AlF_6, Al+AlF_3, Al+$XeMgF_2$, and bare Al as reference samples, were flown onboard the International Space Station (ISS) as part of the Materials International Space Station Experiment 20 (MISSE-20). The MISSE platform is operated by Aegis Aerospace for relatively long-duration (e.g. 6 months) external exposure experiments in a space environment. The coatings were deposited on ULE and Zerodur substrates, and witness samples deposited on the same coatings runs, but on glass slides were left on Earth as control. A subset of the flight samples were fitted with MgF_2 windows to reduce direct exposure to atomic oxygen (AO) and charged particles, and still let through UV and other types of radiation on these samples. After approximately 6 months of exposure in the forward-facing (RAM) direction, the samples were returned to Earth and characterized by performing FUV/NUV/VIS/NIR reflectance measurements to quantify degradation, spectroscopic ellipsometry to evaluate coating thickness and optical constants, atomic force microscopy (AFM) to quantify surface roughness evolution during the flight in the ISS. The MgF_2 protective windows were also analyzed through FUV transmission measurements. Comparison with the witness samples left on the ground and with the flown bare Al samples (with just the naturally occurring Al_2O_3 layer) provided a quantitative assessment of coating thickness variations, optical performance degradation, and morphological changes induced by prolonged exposure to the LEO environment.

Keywords: Far Ultraviolet (FUV), Reflectance, Aluminum (Al), MISSE-20, ISS

1. INTRODUCTION

Protected Al coatings remain the baseline ultraviolet mirror technology for many NASA missions because they combine the high-visible and near-ultraviolet reflectance of aluminum with the excellent far-ultraviolet (FUV) transmission of fluoride overcoats. One of these potential missions is The Habitable Worlds Observatory (HWO), NASA's flagship infrared/optical/ultraviolet mission concept recommended by the 2020 Decadal Survey.[1] The

Further author information: Send correspondence to
M.A.Q.: E-mail: manuel.a.quijada@nasa.gov, Telephone: +1 301 286 3544.

HWO mission will require broadband mirror coatings (at least on the primary/secondary mirrors) with high reflectance from approximately 100 nm to 2.5 μm, while keeping environmental durability and compatibility with high-contrast coronagraph instrumentation. Therefore, the development of resilient, high-performance optical coatings have been identified as one of the enabling technologies for the mission. However, despite several years in the development of several Al-based FUV coatings, there is limited information regarding the long-term stability of these coatings under the combined effects of the Low Earth Orbit (LEO) environment, including ultraviolet radiation, charged particles, thermal cycling, contamination, and atomic oxygen (AO). The AO forms when diatomic oxygen is photo-dissociated by short-wavelength UV radiation from the sun. Atomic-oxygen erosion of optical coatings in LEO poses a serious threat to spacecraft performance and durability. The understanding of how different fluoride protection technologies respond to prolonged exposure to the space environment is therefore critical for qualifying future Al-based optical coatings for long-duration space missions. To investigate the environmental durability of protected aluminum mirror coatings, a flight experiment was conducted as part of the Materials International Space Station Experiment (MISSE-20) onboard the International Space Station (ISS). The experiments included several representative protected aluminum technologies covering both conventional and new fluoride coatings, most of them developed at GSFC in collaboration with other institutions, such as the Naval Research Laboratory (NRL) and the Jet Propulsion Laboratory (JPL): Al+XeLiF, Al+eLiF, Al+Li_3AlF_6, Al+AlF_3, Al+XeMgF_2, and unprotected aluminum as reference samples. The lithium-based (LiF) coatings were included because of their potential to provide FUV reflectance down to 100 nm (Al+eLiF and Al+XeLiF). We also included Al protected with a Li_3AlF_6 overcoat because this material provides the highest reflectance at the H-Lyman α line (Al+Li_3AlF_6),[2] while Al+XeMgF_2 represented a higher Technology Readiness Level (TRL) coating with a known stable protective technology used in the Hubble Space Telescope.[3,4] The aluminum protected with AlF_3 (which has a slightly shorted cut-off wavelength when compared to MgF_2) is seen as a compromise between the stability of MgF_2 and the hygroscopic nature and less environmental stability of LiF (which offers coverage down to 100 nm). Bare aluminum samples were used as controls to evaluate the degradation expected in the absence of a protective fluoride layer. The coated samples were deposited on ULE and Zerodur substrates to investigate whether substrate material influenced the post-flight behavior of the coatings. Also, witness samples fabricated simultaneously on microscope glass slides were retained on Earth to serve as control samples to compare with the ones that flew in space. A total number of 30 samples were included in the experiment, while a selected group of 15 were fitted with a protective MgF_2 window to shield them from direct exposure to AO and charged particles and in order to discriminate from other degradation mechanisms associated with the LEO environment.

2. MISSE-20 EXPERIMENT

As mentioned above, the purpose of the MISSE-20 experiment is to obtain accurate information of passive samples exposed to AO, radiation, and other damaging elements in space to combine with ground measurements to accurately calculate the effect of space environments on different Al-based coatings exposed to the LEO space environment. Optical elements in the LEO environment (between 200 and 2000 km above the surface of the Earth) endure extremely harsh conditions, including exposure to UV, X-ray, and charged-particle radiation; micro-meteoroids and debris. Optical coatings operating in LEO are exposed to a uniquely harsh environment, where multiple degradation mechanisms act simultaneously. One of the most aggressive agents is AO, which can chemically erode exposed materials, modify surface chemistry, increase roughness, and degrade optical performance, particularly in the ultraviolet. In addition, continuous solar ultraviolet radiation and energetic charged particles can induce photochemical changes, create structural defects and color centers in dielectric materials, and alter their optical constants over time. The repeated transitions between sunlight and darkness also subject coatings to severe thermal cycling, producing mechanical stresses due to the coefficient of thermal expansion mismatch between the coating and substrate, which may eventually lead to cracking, delamination, or other morphological changes.

Besides these environmental effects, contamination and particle impacts also contribute to coating degradation. Molecular contaminants originating from spacecraft out-gassing can condense on optical surfaces and, under UV irradiation, form absorbing carbonaceous films that reduce reflectance and transmission, particularly in the FUV.[4] At the same time, impacts from micro-meteoroids and orbital debris can create permanent surface

Table 1: Timeline for the MISSE-20 experiments.

Milestone	Date	Notes
Integration of Al-based coatings in the MISSE-20 carrier at Aegis Aerospace	May 7, 2024	Two members of our team (LRM and MB) traveled to Aegis to assist during sample integration in the MISSE-20 carrier.
SpaceX-31 (SpX-31) Launch with the MISSE-20 carrier	November 5, 2024	NASA launch to deliver carrier to the ISS.
MISSE-20 Installed on ISS	Few days after November 5, 2024	Sample carrier installed on the MISSE Flight Facility (MISSE-FF) forward-facing (RAM) position.
MISSE-20 removal from MISSE-FF	April 28, 2025	Samples were removed after their flight in the ISS.
SpX-32 Splashdown	May 24, 2025	Dragon safely returned to Earth with the MISSE-20 Science Carrier onboard.
MISSE-20 Carrier Returned to Aegis Aerospace	June 20, 2025	Carrier transported back to the Aegis facility following recovery.
De-integration at Aegis Aerospace facility	June 24-25, 2025	LRM and MB went to Aegis again to assist during de-integration and bring samples back to GSFC for post-flight characterization.

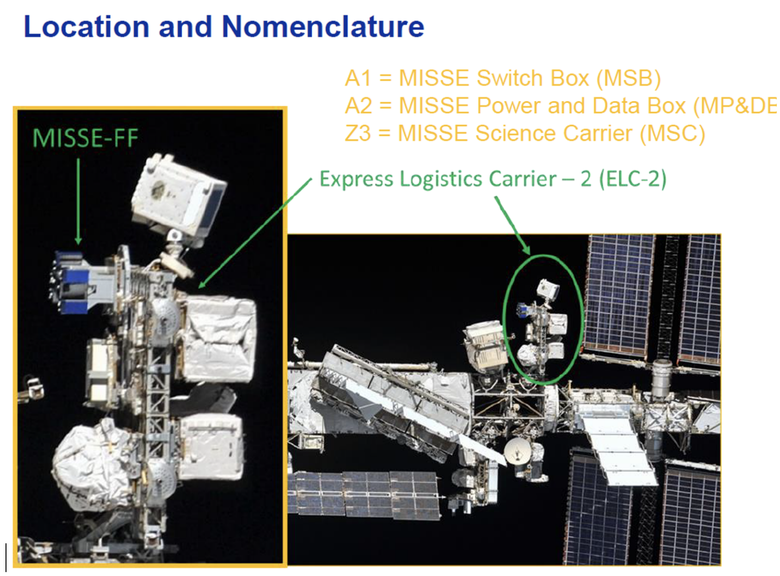

Figure 1: Location of the MISSE carrier on the ISS.

defects such as pits and craters, increasing scattering losses and degrading optical quality. While orbital debris in LEO typically ranges from approximately 10 μm to 1 mm in size, natural micro-meteoroids are generally more damaging because of their higher impact velocities. The combined action of all these mechanisms can significantly reduce optical performance, making long-duration flight experiments such as the ones reported in this work essential for evaluating the environmental durability of advanced optical coating technologies under realistic space conditions.

The various coating technologies reported in this work are specifically designed to meet HWO requirements, which are intended for operation at the Earth-Sun Lagrange (L2) orbit where the environmental conditions are expected to be milder than LEO. However, these coatings will be briefly exposed to LEO environments during the flight to the L2 orbit. Therefore, long-term survivability in LEO is likely a sufficient condition to expect survivability in LEO (a few hours to a day) plus several years at L2. The 30 samples based on the aforementioned coatings flew in the ISS for a period of 6 months. These were part of the MISSE-20 experiments that are operated by Aegis Aerospace, which owns the MISSE platform that is permanently installed on the ISS truss near the solar arrays (ELC 2, Site 3, Fig. 1). This facility offers a unique opportunity for external orbital testing of a wide range of technologies in a microgravity environment and it provides exposure to all four directional faces. The experimental timeline are shown in Table 1. Following retrieval from the ISS and de-integration, the samples underwent post-flight characterization at GSFC. Measurements included FUV-NUV-VIS-NIR reflectance to evaluate pre- and post-flight degradation, spectroscopic ellipsometry to determine changes in the fluoride thickness and optical constants, and atomic force microscopy (AFM) to quantify surface roughness over multiple spatial scales. The protective MgF_2 windows were also characterized by FUV transmission measurements to assess possible degradation of the windows themselves during the mission. Comparison with the witness samples that remained on the ground allowed for quantitative analysis of coating thickness variations, reflectance degradation and morphological changes associated with long-term exposure to the LEO environment.

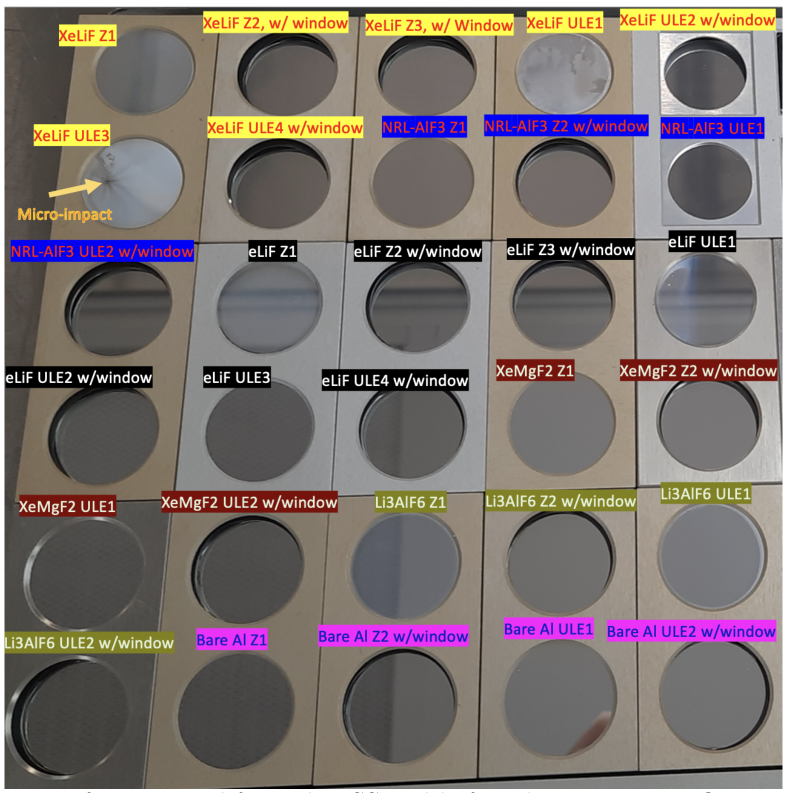

Figure 2: MISSE-20 carrier after retrieval from the ISS and before de-integration. One sample (second row from top left corner) shows the impact of a micro-meteorite. ULE and Z (Zerodur) are the substrates used for each individual sample. Samples labeled "w/window" were flown behind a MgF_2 protective window.

3. SAMPLES PREPARATION AND CHARACTERIZATION

A total of 30 coated samples were prepared for the MISSE-20 flight experiment. The sample deposition techniques had been described elsewhere.[5–11] The experiments were designed so that approximately half of the samples were individually protected with MgF_2 windows. These windows were intended to minimize direct exposure to AO and charged particles, but still allow for other types of space radiation to go through. This approach enabled a partial discrimination between degradation mechanisms associated with AO and charged particles and those resulting from ultraviolet radiation, contamination, thermal cycling, and other environmental factors. The samples included protected aluminum coatings deposited on ULE and Zerodur substrates together with witness samples fabricated simultaneously on microscope glass slides and retained on Earth. These witness samples served as control in order to evaluate the performance of the coatings that were part of these MISSE-20 experiments. Figure 2 shows the MISSE-20 carrier immediately after retrieval from the ISS and before sample de-integration. This figure shows in the upper left corner one sample which exhibits a clear micro-meteoroid impact, illustrating one of the degradation mechanisms encountered during the mission. In terms of sample characterization, the reflectance of the mirrors and transmittance of the MgF_2 windows were measured in the FUV range with a McPherson Vacuum Ultraviolet (VUV) 225 spectrometer. This spectrometer has a one-meter-long high-vacuum monochromator with a 1200 lines/mm grating operating at near-normal incidence in the spectral range from 30 nm to 325 nm. The spectrometer is equipped with a windowless hydrogen-purged light source, which provides discrete H_2 emission lines between 90 nm and 160 nm and a continuum above the latter wavelength. Reflectance in the NUV-Vis-NIR was measured with a Perkin Elmer lambda-950 nm. The angle of incidence for the reflectance measurements in either of these spectrometers was 10° from normal incidence. Ellipsometry measurements in the 200−2000 nm range were performed with a HORIBA Jovin-Yvon spectroscopic ellipsometer in a fixed arm configuration of 70°.

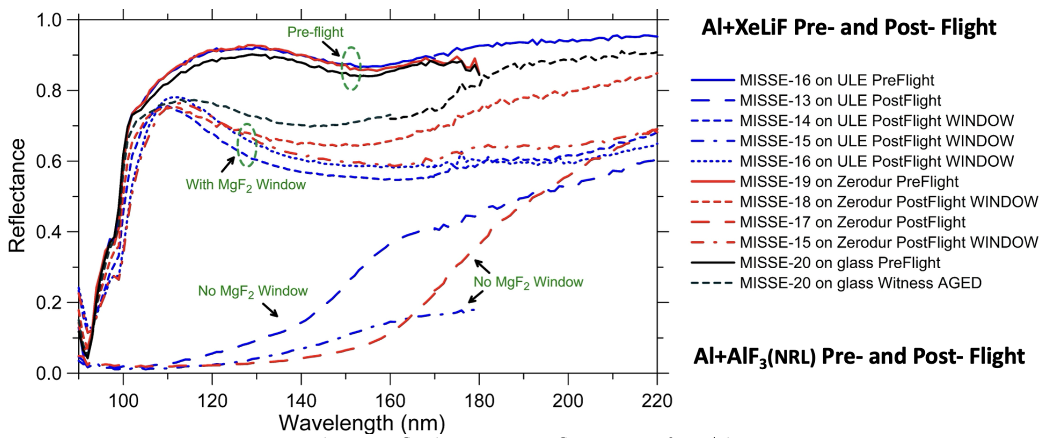

Figure 3: Pre- and Post-flight FUV reflectance for Al+XeLiF coupons.

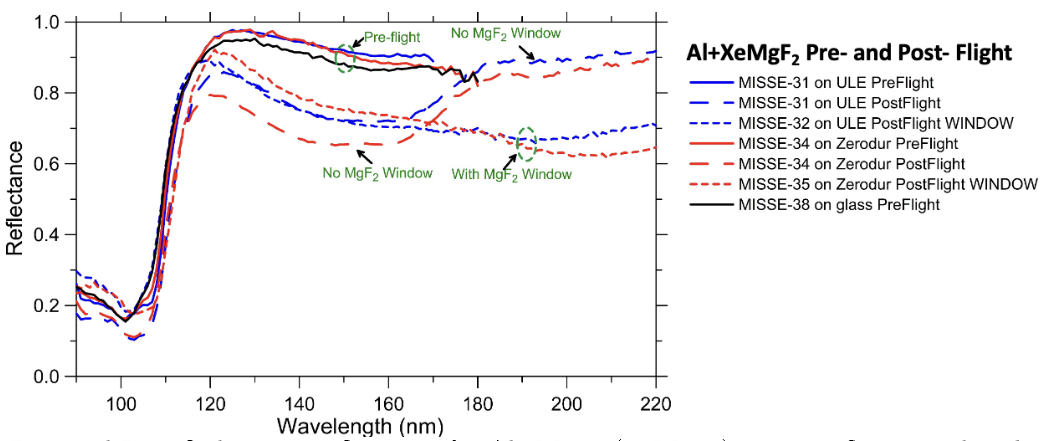

Figure 4: Pre- and Post-flight FUV reflectance for Al+MgF_2 ($XeMgF_2$) coupons fluorinated with XeF_2 gas.

4. RESULTS

4.1 FUV Reflectance Pre- and Post-Flight

The methodology in these FUV reflectance experiments was to measure the pre- and post-flight reflectance in each of these samples that were part of the MISSE-20 experiments. The results of these are shown in Figures 3−8. For example, Figures 3 and 4 show the pre- and post-flight FUV reflectance for the Al+XeF_2+LiF (XeLiF) and

Al+XeF_2+MgF_2 ($XeMgF_2$) samples respectively. The results are that the $XeMgF_2$ samples[5] fared the best, in terms of maintaining their pre- and post-flight reflectance. These results show that $XeMgF_2$ (specifically for samples fitted with the MgF_2 window) retained a high reflectance after the 6 months flight in the ISS. The average post-flight reflectance was approximately $> 80\%$ in the FUV (typically with only $< 10\%$ loss) whereas samples directly exposed (without window) experienced a degradation in the $10-17\%$ range. The Al+AlF_3 samples prepared in the Large Area Plasma Processing System (LAPPS) at NRL[6,7] also had good performance as they degraded significantly less (average R $> 70\%$) when compared to the other types of samples. The pre- and post-flight differences between windowed and windowless samples were slightly larger (when compared to $XeMgF_2$). The Li-based coatings (Al+Li_3AlF_6,[2,8] Al+eLiF,[9,10] and Al+XeLiF[5,11]) exhibited the largest degradations of all the samples as they almost lost the FUV reflectance, specially for those without the MgF_2 window. The differences between windowed and windowless samples were quite large, with windowless samples losing about 80% of their original reflectance. Among these, the Al+Li_3AlF_6 samples performed slightly better as they retained an average FUV reflectance of around 20% (windowless) as shown in the results in Fig. 5. The average FUV reflectance for Al+XeLiF and Al+eLiF samples was $< 20\%$ below 160 nm. Another important observation from these results is that there was not a clear trend of FUV reflectance for bare Al samples (see Fig. 8) regardless of whether they were fitted with or without a MgF_2 window. The last point is that there is little evidence that the choice of ULE or Zerodur substrate made a clear difference in any of these samples, regardless of which coating technology was applied to these two types of substrates. The following section discusses how the reflectance in the UV/Visible/NIR spectral regions was impacted for the samples that flew in the MISSE-20 experiments.

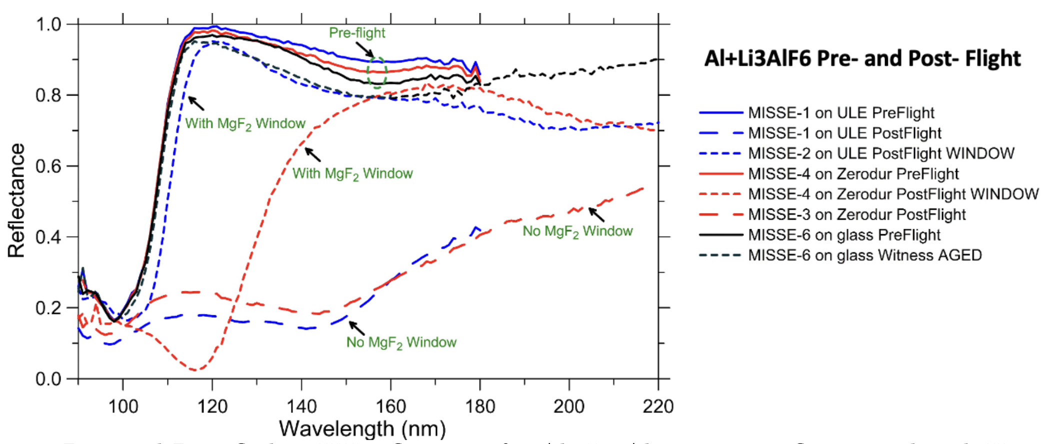

Figure 5: Pre- and Post-flight FUV reflectance for Al+Li_3AlF_6 coupons fluorinated with XeF_2 gas.

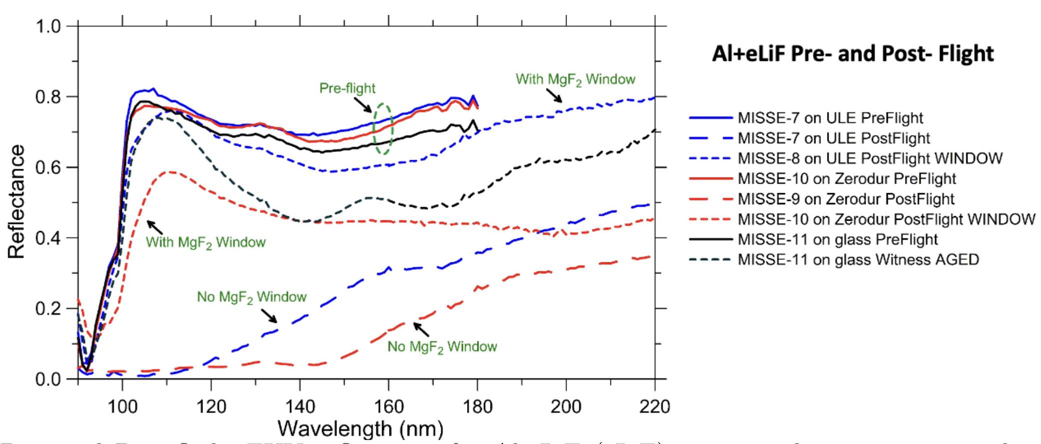

Figure 6: Pre- and Post-flight FUV reflectance for Al+LiF (eLiF) coupons that were prepared with the hot process and capped with an ALD layer of MgF_2.

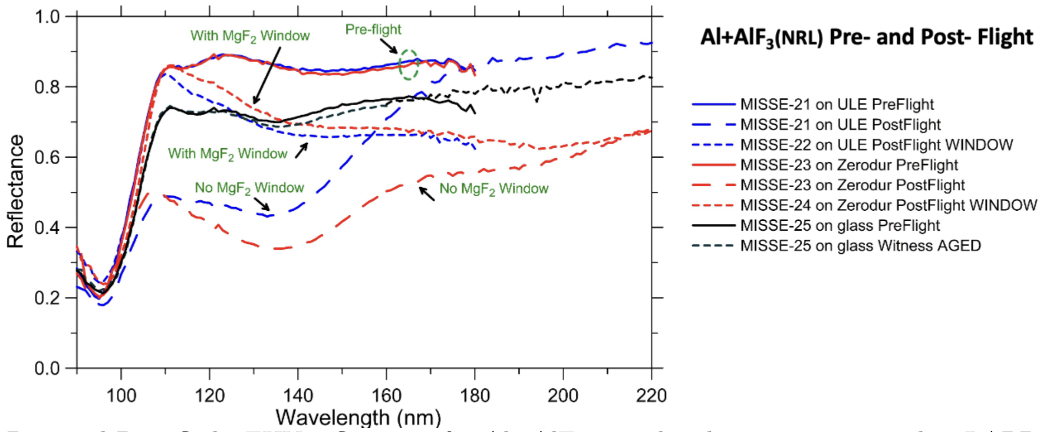

Figure 7: Pre- and Post-flight FUV reflectance for Al+AlF_3 samples that were processed in LAPPS at NRL.

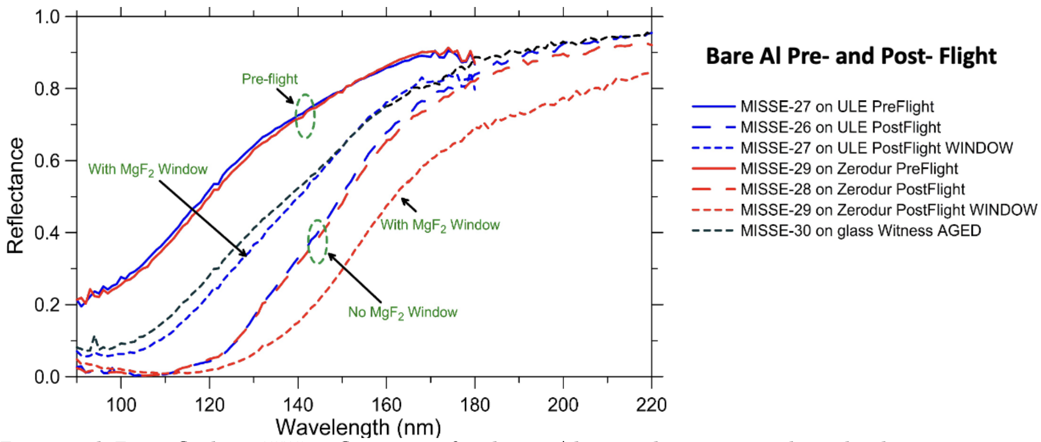

Figure 8: Pre- and Post-flight FUV reflectance for bare Al samples prepared with the conventional Physical Vapor Deposition process.

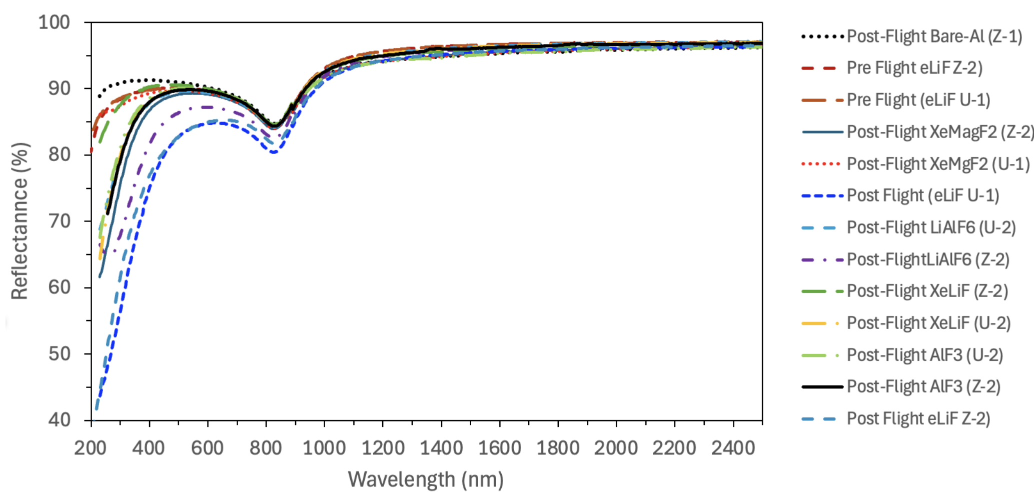

Figure 9: Pre- and Post-flight FUV reflectance data comparison in the NIR/Visible/UV spectral ranges.

4.2 NIR/Vis/UV Reflectance Pre- and Post-Flight

Figure 9 displays representative data for each of the coating technologies for which FUV reflectance was discussed in Section 4.1. The samples selected for this figure were equipped with the protective MgF_2 window, since this minimized excessive AO exposure during flight. The reflectance behavior in the NIR spectral range (800−2500 nm) is nearly the same for all samples pre- and post-flight. The behavior in the Visible/UV ranges (200−800 nm) falls in roughly 3 categories. The first group includes samples for which the post-flight results were similar to the pre-flight data with an average reflectance of 85-90 % in the 200−400 nm range. This group includes the bare Al as well as the $XeMgF_2$ samples which retained their FUV reflectance (as shown in Fig. 4). The second group is for samples with an UV reflectance average of around 60% in the same 200−400 nm range. The last group includes the post-flight data for the eLiF samples for which the reflectance dropped to 40 % at 200 nm. The eLiF samples were the ones with the most degradation in this region and this is consistent with the FUV reflectance degradation shown in Fig. 6. The next section will focus on how the reflectance losses correlated with the Atomic Force Microscope (AFM) measurements performed on these samples.

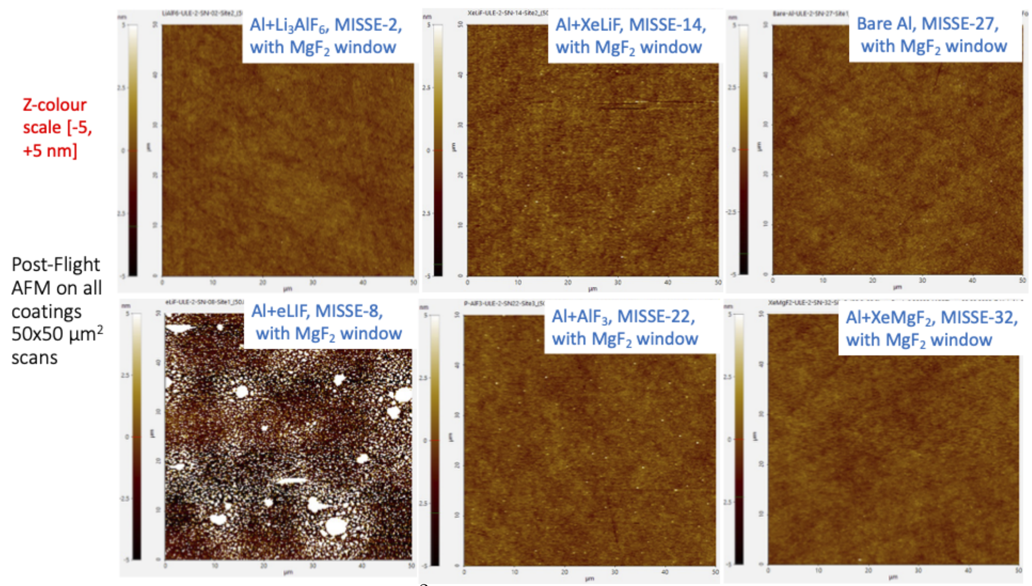

Figure 10: Post-flight AFM scans (50×50 μm^2 area) taken on samples representative of each of the coating technologies discussed in this work. All the AFM scans correspond to samples flown with the protective MgF_2 window.

4.3 AFM Measurements Pre- and Post-Flight

We performed AFM measurements on each of these samples. The data were obtained for each sample with scan sizes of 10×10 μm and 50×50 μm. Each scan size for each sample was measured at 3 different locations, and then averaged. The AFM tip had a radius of 10 nm, and data were collected in the tapping mode. The Al+AlF_3 and bare Al exhibited the best results with the smallest variation and excellent agreement with their corresponding witnesses left on the ground, even without the presence of a MgF_2 protective window. The Al+$XeMgF_2$ samples also show excellent stability, but samples without protective MgF_2 windows have slightly higher roughness values. The Li-based coatings (Al+Li_3AlF_6, Al+eLiF, and Al+XeliF) presented significant surface morphology changes after flight. The post-flight deviations from their witness samples are significantly larger when compared to bare Al, AlF_3 or MgF_2 coatings. The degradation affects a wide range of spatial frequencies, meaning that the LEO exposure basically impacts the coating at different frequencies. The use of MgF_2 protective windows seems to have a positive impact on the roughness variation. This means that the most probable source of degradation is AO, contamination, charged particles, or a combination of all of these. The thermal cycling and UV radiation should still be present even with the MgF_2 windows. Overall, samples protected with the window showed smaller post-flight roughness increase compared to their corresponding witnesses left

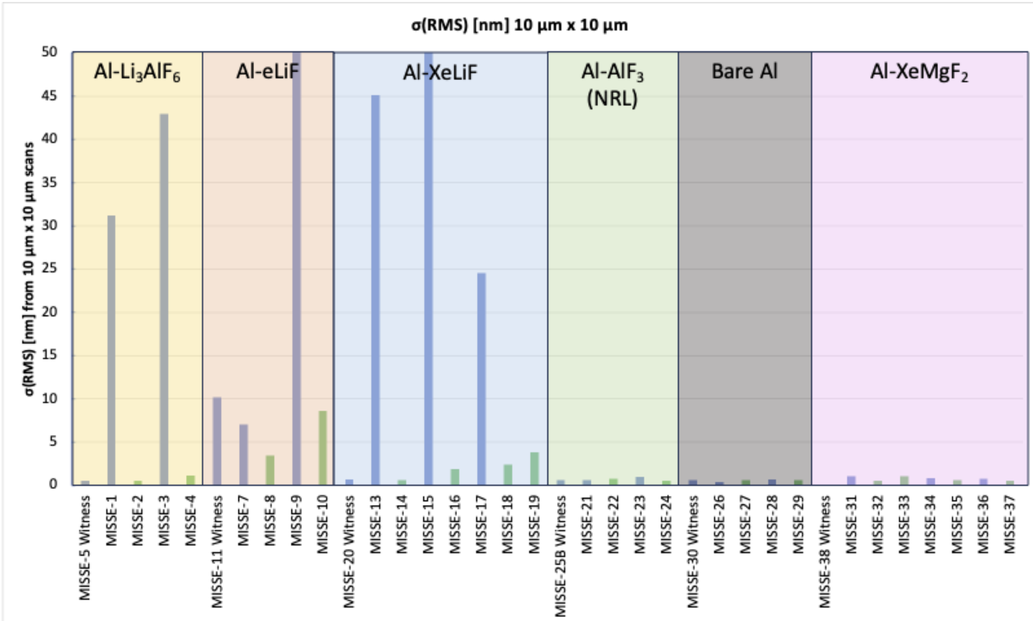

Figure 11: Pre- and Post-flight roughness variation based on the 10×10 μm^2 AFM scans for the samples used in this study. The green columns correspond to the samples flown with the protective MgF_2 window, while the blue columns correspond to samples without it.

on the ground. The substrate choice (ULE or Zerodur) did not show a clear effect on how the AFM results were impacted in all these samples. These data confirm strong correlation between roughness and "increases" in overcoat thicknesses measured via ellipsometry, suggesting the latter are basically artifacts originated from changes in surface morphology. More importantly, two independent metrologies (AFM and ellipsometry) hint at the same possible effect: Direct exposure to LEO, in the RAM direction, induces a dominant micro-structural evolution in Li-based coatings, but AlF_3 or $XeMgF_2$ overcoats, and bare Al remained more stable.

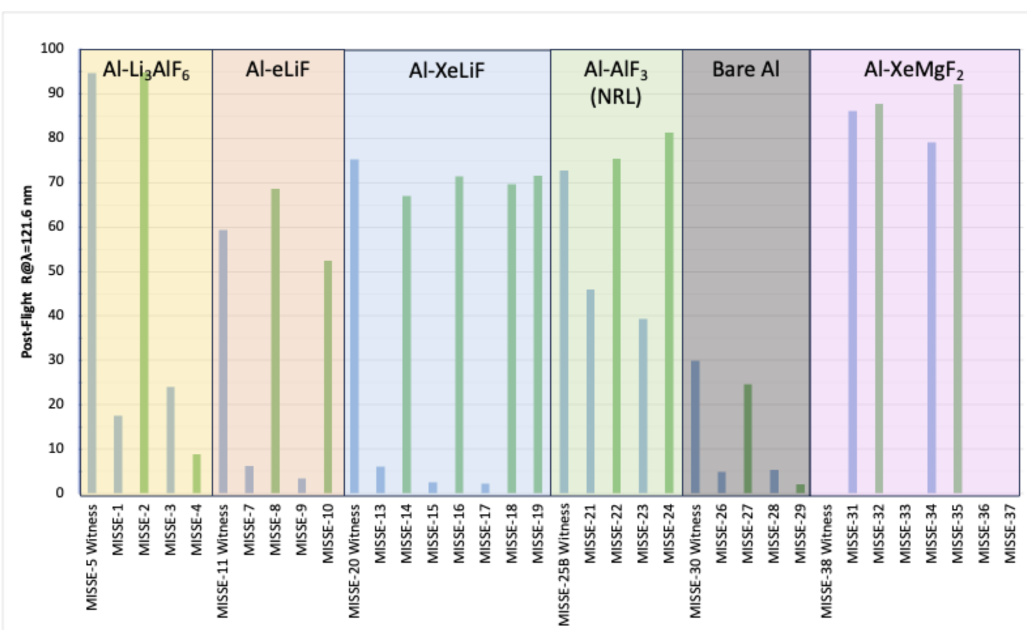

Figure 12: Thickness variation compared to witnesses kept on Earth. The green columns correspond to the samples flown with the protective MgF_2 window, while the blue columns correspond to samples without it.

4.4 Thickness Variations from Ellipsometry of Post-Flight Samples

Figure 12 shows the thickness variations for all samples that were flown in the MISSE-20 experiments. The thickness parameters were obtained by ellipsometric fits. Since apparent ”thickness changes” could actually reflect changes in refractive index or coating structure, the optical properties (n,k) of each fluoride was fitted along with the coating for each corresponding witness coupon kept on the ground. Then, the n,k used for fitting the samples that flew on MISSE-20 were fixed (not fitted), and were the same for each coating technology. We concluded that there was little evidence that the ISS environment (RAM direction) removed fluoride material. In fact, we noticed the measured thicknesses are mostly larger than those of the witnesses. The apparent post-flight apparent increase in thickness also correlates with an increase in surface roughness (see Section 4.3) and this suggests the measured thickness deviations are mostly due to changes in surface morphology. There could also be a carbon-based contamination growth, as suggested in Section 4.5 below. The results shown in Fig. 12 indicate that the Al+AlF_3 samples showed the best behavior (even better than bare Al), with the smallest variation and with excellent agreement with the thickness of the witness sample left on Earth. The Li-based coatings (Al+Li_3AlF_6, Al+eLiF, Al+XeliF) present significant thickness variation. The post-flight deviations from their witness samples are significantly larger when compared to bare Al, AlF_3 or MgF_2 coatings. This trend for all Li-containing coatings may be due to the intrinsic properties of Li-based fluorides rather than specific coating process or the substrate of choice. The use of MgF_2 protective windows seem to have an impact on the thickness variation. Overall, samples protected with the MgF_2 windows show smaller post-flight thickness ”growth” when compared to their witnesses left on Earth. In addition, the substrate choice (ULE or Zerodur) did not show a clear impact or trend in these results.

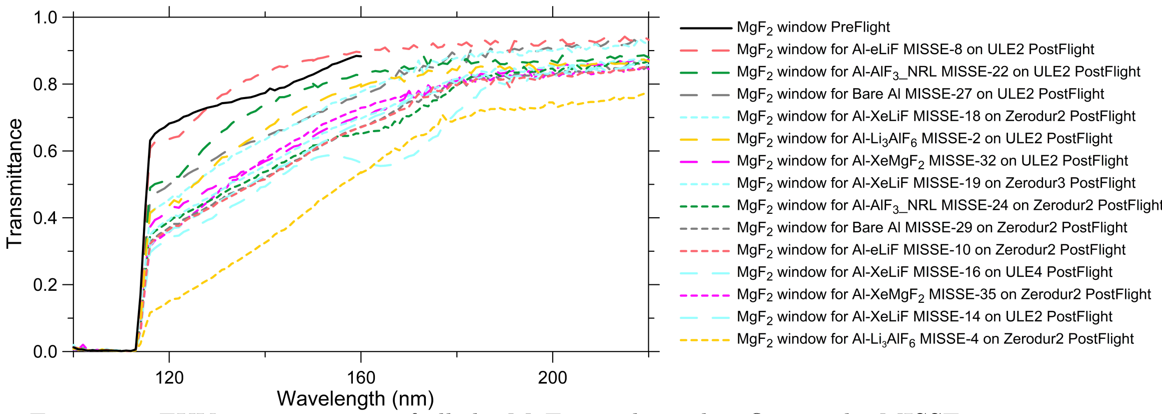

Figure 13: FUV transmittance of all the MgF_2 windows that flew in the MISSE-20 experiment.

4.5 Spectral Transmittance of MgF_2 Windows

Figure 13 shows the transmittance of all the MgF_2 windows (1” diameter, 1 mm thick) used to protect a selected group of protected Al samples that flew in the ISS. This figure shows the transmittance of just one representative MgF_2 window (black curve) prior to the flight in the ISS. It should be noted that the data for all pre-flight MgF_2 windows displayed similar results as the black curve in Fig. 13. Once all samples were returned from space, we re-measured their FUV transmittance to compare to the post-flight data. The first observation is that we did not find a clear correlation between the measured transmission and the physical location of the windows in the MISSE-20 carrier (see Fig. 2). Furthermore, it is unclear if the experimental setup may have contributed to the non-uniform degradation observed across all the samples shown in Fig. 13. We observe that aside from one sample (which did not show any degradation) most of the windows suffered severe degradation, with most displaying about 50% reduction near the 120 nm wavelength. These results suggest the LEO environment and conditions seem to be very deleterious to these MgF_2 samples, in spite of the fact that they are single crystals. Our hypothesis is that AO and space radiation (energetic particles and UV) could have caused significant damage to the MgF_2. This may explain the large difference in reflectance between Al-based coatings flown with and without MgF_2 protective window. In addition, two of the windows show a noticeable dip in transmittance at around 160 nm. This dip may suggest the changes seen in some of these windows may have originated from carbon-based contamination, since it occurs well into the UV to be caused by colour centers.

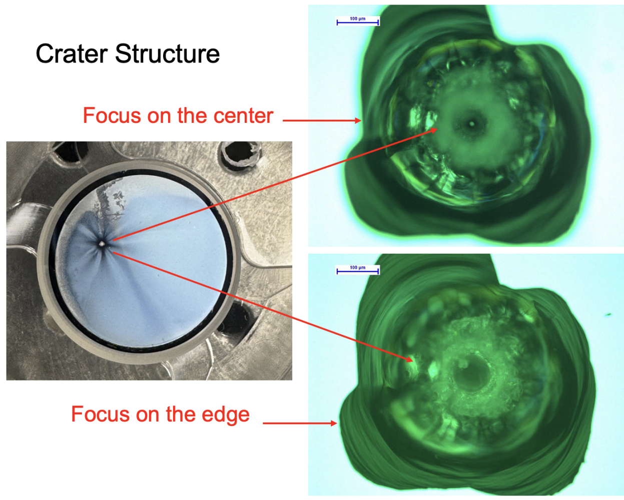

Figure 14: Closer look at the impact site on the XeLiF sample that occurred during flight.

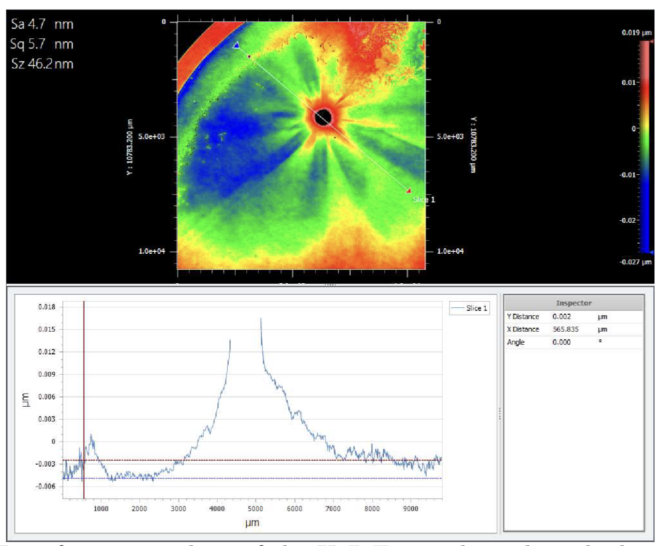

Figure 15: Interferometric data of the XeLiF sample with with the impact site.

4.6 Closer Look at Meteorite Impact Crater

We will now take a closer look at the micro-meteorite impact location on the XeLiF sample labeled as XeLiF ULE3 that is shown in the upper left corner of Fig. 2. Figure 14 shows the structure of the crater at two focal points near the center of the impact and at the edges. We estimated that the diameter of the core is about 10 μm, while the crater diameter is about 500 μm. Although the depth of the impact did not go all the way through the ULE substrate, it was certainly deeper than the depth of focus of the objective used for collecting the images shown in this figure. It is interesting to note that the two focusing images showed different structures as we went through these two focus positions and this suggests very localized damages on the coated XeLiF layers of the sample. We now turn our attention to the interferometric data that are shown in Fig. 15. The area in this figure is 10 mm $\times$ 10 mm and it was created by stitching various scans of smaller sizes. The line scan performed along the center of the crater indicates the crater height increases near the edge. Furthermore, the degradation is uniform around the crater and it exhibits a circular symmetry. The crater depth information is lost because it extends beyond the vertical range of the objective used for collecting the data shown in Fig. 15. In sum, this figure indicates the damages caused by the impact are mostly confined within the mirror coating. The damages on this XeLiF mirror coupon with a micro-meteorite impact show as a ripple effect in the coating flowing outward from the center of the impact. Further away from the impact, the surface RMS is degraded. Although this is not due to the impact, but rather surface morphology changes as suggested in Section 4.5. This sample has a visible haze since it did not have the MgF_2 protective window and therefore, the sample exhibits a severely degraded reflectance in the UV and Visible spectral ranges.

5. CONCLUSION

In summary, these MISSE-20 experiments have provided valuable information on the effect on various types of FUV coating technologies on samples exposed to AO, radiation, and other damaging elements in the LEO orbit that when combined with ground measurements allowed us to accurately calculate the effect on these samples from space environments. These coatings were exposed to the LEO space environment for a period of six months (between 200 and 2000 km above the surface of the Earth) and they endured extremely harsh conditions, including exposure to UV, X-ray, and charged-particle radiation; micro-meteoroids and debris. The coating technologies discussed in this work are specifically designed to meet HWO requirements, which are intended for operation at the Earth-Sun Lagrange (L2) orbit, where the concentration of one of the more damaging radiation elements (such as AO) is expected to be much smaller. However, these MISSE-20 experiments are still providing invaluable information as the optical coatings will be briefly exposed to LEO during the flight to L2.

ACKNOWLEDGMENTS

Financial support is through a GSFC Internal Research and Analysis (IRAD) grant and a NASA Strategic Astrophysics Technology (SAT) grant No. 21-SAT21-0027 and Astrophysical Research and Analysis (APRA) grant No. 22-APRA22-0027. LRM acknowledges the support of CRESST II cooperative agreement, supported by NASA under award number 80GSFC21M0002.

REFERENCES

[1] National Academies of Sciences, Engineering, and Medicine 2021 in [*Pathways to Discovery in Astronomy and Astrophysics for the 2020s*], The National Academies Press, Washington, DC (2021).

[2] Javier Del Hoyo, Luis Rodriguez-de-Marcos, John Hennessy, M. Batkis, Caleb Bos, Manuel Quijada, "Cryolite overcoated aluminum reflectors for far-ultraviolet spectroscopy," *International Society for Optics and Photonics* **12676**, 126760I (2023).

[3] R.A.M. Keski-Kuha, J.L. Larruquert, J.S. Gum, and C.M. Fleetwood, "Optical coatings and materiasl for ultraviolet space applications," in [*in [Ultraviolet-Optical Spoace Astronomy Beyond HST]*], 406–419, J. A. Morse, J. M. S. and Kinney, A. L., eds., ASP Conference 164 (1999).

[4] M. A. Quijada, R. M. Henry, T. Madison, R. Boucarut and J. G. Hagopian, "Post-Flight Reflectance of COSTAR and WF/PC 2 Pickoff Mirrors Upon Their Return from Space," *Proc. of SPIE* **7739** (2010).

[5] Manuel A. Quijada, Luis V. Rodriguez de Marcos, Javier G. Del Hoyo, Emrold Gray, Edward J. Wollack, Ari Brown, "Advanced Al mirrors protected with LiF overcoat to realize stable mirror coatings for astronomical telescopes," *Proc. SPIE, Advances in Optical and Mechanical Technologies for Telescopes and Instrumentation V,* **121881**, 121881V (2022).

[6] L. V. Rodríguez De Marcos, J. I. Larruquert, J. A. Méndez, N. Gutiérrez-Luna, L. Espinosa-Yáñez, C. Honrado-Benítez, J. Chavero-Royán, and B. Perea-Abarca, "Optimization of MgF2-deposition temperature for far UV Al mirrors," *Opt. Express* **26**, 9363–9372 (2018).

[7] L. V. Rodriguez de Marcos, D. R. Boris, E. Gray, J. G. del Hoyo, A. C. Kozen, J. G. Richardson, S. G. Rosenberg, S. G. Walton, V. Wheeler, E. J. Wollack, J. M. Woodward, and M. A. Quijada, "Room temperature plasma-etching and surface passivation of far-ultraviolet Al mirrors using electron beam generated plasmas," *Opt. Mater. Express* **11**, 740–756 (2021).

[8] Javier Del Hoyo, Luis Rodriguez de-Marcos, M. Batkis, and Manuel Quijada, "Optimization of mission enabling broadband Lyman ultraviolet series to infrared aluminum lithium fluoride reflectors," *Proc. SPIE* **13100-81**, In Press (2024).

[9] B. Fleming, M. Quijada, J. Hennessy, A. Egan, J. Del Hoyo, B. A. Hicks, J. Wiley, N. Kruczek, N. Erickson, and K. France, "Advanced environmentally resistant lithium fluoride mirror coatings for the next generation of broadband space observatories," *Appl. Opt.* **56**, 9941–9950 (2017).

[10] L. Rodríguez-de Marcos, B. Fleming, J. Hennessy, *et al.*, "Advanced Al/eLiF mirrors for the SPRITE CubeSat," *Proc. SPIE 12188, Advances in Optical and Mechanical Technologies for Telescopes and Instrumentation V* **12188**, 740–756 (2022).

[11] Manuel A. Quijada, Javier G. Del Hoyo, Luis V. Rodriguez De Marcos, Edward J. Wollack, Mateo F. Batkis, Devin M. Lewis, Tanner D. Rydalch, David D. Allred, "Far-ultraviolet optical properties and performance of physical vapor deposited aluminum mirrors protected with XeLiF and $XeMgF_2$," *Journal of Astronomical Telescopes, Instruments, and Systems* **11**, 042209 (2025).